SUPER RESOLUTION OF MULTISPECTRAL IMAGES USING LOCALLY ADAPTIVE MODELS

Rafael Molina[1], *Javier Mateos*[1], *Miguel Vega*[2], *and Aggelos K. Katsaggelos*[3]

1. Departamento de Ciencias de la Computación e I.A., Universidad de Granada, 18071 Granada, Spain
email: {rms, jmd}@decsai.ugr.es
2. Departamento de Lenguajes y Sistemas Informáticos, Universidad de Granada, 18071 Granada, Spain
email: mvega@ugr.es
3. Department of Electrical Engineering and Computer Science, Northwestern University
2145 Sheridan Rd, Evanston, IL 60208-3118, USA
email: aggk@ece.northwestern.edu

ABSTRACT

In this paper we present a locally adaptive super resolution Bayesian methodology for pansharpening of multispectral images. The proposed method incorporates prior local knowledge on the expected characteristics of the multispectral images, uses the sensor characteristics to model the observation process of both panchromatic and multispectral images, and includes information on the unknown parameters in the model in the form of hyperprior distributions. Using real and synthetic data, the pansharpened multispectral images are compared with the images obtained by other parsharpening methods and their quality is assessed both qualitatively and quantitatively.

1. INTRODUCTION

Nowadays most remote sensing systems include sensors able to capture, simultaneously, several low resolution images of the same area on different wavelengths, forming a multispectral image, along with a high resolution panchromatic image. The main characteristics of such remote sensing systems are the number of bands of the multispectral image and the resolution of those bands and the panchromatic image. For instance, the Landsat 7 satellite (http://landsat.gsfc.nasa.gov/), equipped with the ETM+ sensor, allows for the capture of a multispectral image with six bands (three bands on the visible spectrum plus three bands on the infrared) with a resolution of 30 meters per pixel, a thermal band with a resolution of 60 meters per pixel and a panchromatic band (covering a large zone on the visible spectrum and the near infrared), with a resolution of 15 meters per pixel.

The main advantage of the multispectral image is to allow for a better land type and use recognition but, due to its lower resolution, information on the objects' shape and texture may be lost. On the other hand, the panchromatic image allows for a better recognition of the objects in the image and their textures but provides no information about their spectral properties.

Throughout this paper the term *multispectral image reconstruction* will refer to the joint processing of the multispectral and panchromatic images in order to obtain a new multispectral image that, ideally, will exhibit the spectral characteristics of the observed multispectral image and the resolution and quality of the panchromatic image. The use of such an approach, also named pansharpening, will allow us to obtain, in the case of Landsat 7 ETM+, a multispectral image with a resolution of 15 meters per pixel.

A few approximations to multispectral image reconstruction have been proposed in the literature. See, for instance, [1, 2, 3, 4, 5, 6]. Recently a few super-resolution based methods have also been proposed. Eismann and Hardie [7] proposed a MAP approach that makes use of a stochastic mixing model of the underlying spectral scene content to achieve resolution enhancement beyond the intensity component of the hyperspectral image. Akgun *et. al.* [8] proposed a POCS based algorithm to reconstruct hyperspectral images where the hyperspectral observations from different wavelengths are represented as weighted linear combinations of a small number of basis image planes.

In this paper we follow the hierarchical Bayesian in providing a solution to the super resolution reconstruction of multispectral images problem and include as a part of the innovation of the proposed approach the utilization of spatially varying image models. Then, by applying variational methods to approximate probability distributions we estimate the unknown parameters, and the high resolution multispectral image.

The paper is organized as follows. In section 2 the Bayesian modeling and inference for super resolution reconstruction of multispectral images is presented. The required probability distributions for the Bayesian modeling of the super resolution problem are formulated in section 3. The Bayesian analysis and posterior probability approximation to obtain the parameters and the super resolution reconstructed image is performed in section 4. Experimental results on a real Landsat 7 ETM+ image are described in section 5 and, finally, section 6 concludes the paper.

2. BAYESIAN PROBLEM FORMULATION

Let us assume that $\mathbf{y}$, the multispectral image we would observe under ideal conditions with a high resolution sensor, has B bands $\mathbf{y}_b$, $b = 1,\ldots,B$, that is,

$$\mathbf{y} = [\mathbf{y}_1^t, \mathbf{y}_2^t, \ldots, \mathbf{y}_B^t]^t,$$

where each band is of size $p = m \times n$ pixels and t denotes the transpose of a vector or matrix. Each band of this image is expressed above as a column vector by lexicographically ordering the pixels in the band.

In real applications, this high resolution image is not available. Instead, we observe a low resolution multispectral image $\mathbf{Y}$ with B bands $\mathbf{Y}_b$, $b = 1,\ldots,B$, that is,

$$\mathbf{Y} = [\mathbf{Y}_1^t, \mathbf{Y}_2^t, \ldots, \mathbf{Y}_B^t]^t,$$

where each band is of size $P = M \times N$ pixels with $M < m$ and $N < n$. Each band of this image is also expressed as a column vector by lexicographically ordering the pixels in the band.

The sensor also provides us with a panchromatic image $\mathbf{x}$ of size $p = m \times n$, obtained by spectrally averaging the unknown high resolution images $\mathbf{y}_b$.

The objective of the high resolution multispectral image reconstruction problem is to obtain an estimate of the unknown high resolution multispectral image $\mathbf{y}$ given the panchromatic high resolution observation $\mathbf{x}$ and the low resolution multispectral observation $\mathbf{Y}$. The Bayesian formulation of this problem requires the definition of the joint distribution $\mathrm{p}(\Omega, \mathbf{y}, \mathbf{Y}, \mathbf{x})$, where Ω denotes the set of hyperparameters needed to describe the required probability density functions.

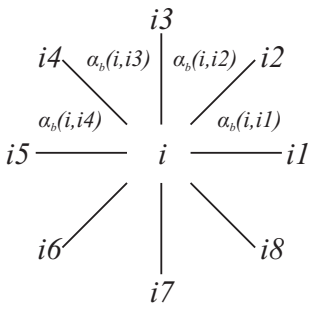

Figure 1: Pixel and inverse variance notation.

For Ω, $\mathbf{y}$, $\mathbf{Y}$, and $\mathbf{x}$ the following joint distribution is defined (we utilize in this paper the hierarchical Bayesian paradigm see, for example, [9]).

$$\mathrm{p}(\Omega,\mathbf{y},\mathbf{Y},\mathbf{x}) = \mathrm{p}(\Omega)\mathrm{p}(\mathbf{y}|\Omega)\mathrm{p}(\mathbf{Y},\mathbf{x}|\mathbf{y},\Omega), \tag{1}$$

and inference is based on $\mathrm{p}(\Omega,\mathbf{y}|\mathbf{Y},\mathbf{x})$.

The distribution $\mathrm{p}(\Omega,\mathbf{y}|\mathbf{Y},\mathbf{x})$ is calculated (approximated) in this paper using variational distribution approximation (see chapter II in [10] for an excellent introduction to variational methods and their relationships to other inference approaches). Recent years have seen a growing interest in the application of variational methods [11, 12] to inference problems. These methods attempt to approximate posterior distributions with the use of the Kullback-Leibler cross-entropy [13]. Applications of variational methods to Bayesian inference problems include, for instance, graphical models and neural networks [11], independent component analysis [12], and blind deconvolution problems [14, 15].

In the coming sections we address the modeling as well as the inference steps in our Bayesian formulation of the super resolution reconstruction of multispectral images.

3. HYPERPRIORS, PRIORS, AND OBSERVATION MODELS USED IN SUPER RESOLUTION MULTISPECTRAL IMAGE RECONSTRUCTION

In this paper we do not use the correlation between different high resolution bands and concentrate on modeling the local variation at each band. In the definition of the image model we use the notation $i1, i2, \ldots, i8$ to denote the eight pixels around pixel i (see Fig. 1). Then following the approximation in [16] which extends Conditional Auto-Regressions [17] to take into account local variability we write

$$\begin{aligned}\mathrm{p}(\mathbf{y}|\Omega) &= \prod_{b=1}^{B}\mathrm{p}(\mathbf{y}_b|\alpha_b)\\ &\propto \prod_{b=1}^{B}\prod_{i=1}^{p}\prod_{l=1}^{4}\alpha_b(i,il)^{1/8}\exp\left\{-\frac{1}{2}\alpha_b(i,il)\left[y_b(i)-y_b(il)\right]^2\right\},\end{aligned} \tag{2}$$

where $\alpha_b(i,il)$ controls, for the b-band, the smoothness of the restoration between pixels i and il and

$$\alpha_b = (\alpha_b(i,il) \mid i = 1,\ldots,p,\ l = 1,\ldots,4).$$

We assume that $\mathbf{Y}$ and $\mathbf{x}$, for a given $\mathbf{y}$ and a set of parameters Ω, are independent and consequently write

$$\mathrm{p}(\mathbf{Y},\mathbf{x}|\mathbf{y},\Omega) = \mathrm{p}(\mathbf{Y}|\mathbf{y},\Omega)\mathrm{p}(\mathbf{x}|\mathbf{y},\Omega)\,. \tag{3}$$

Each band, $\mathbf{Y}_b$, is related to its corresponding high resolution image by

$$\mathbf{Y}_b = \mathbf{D}\mathbf{H}\mathbf{y}_b + \mathbf{n}_b, \quad \forall b = 1,\cdots,B, \tag{4}$$

where $\mathbf{H}$ is a $p\times p$ blurring matrix and $\mathbf{D}$ is a $P\times p$ decimation operator.

Given the degradation model for multispectral image super-resolution described by Eq. (4) and assuming independence between the noise observed in the low resolution images, the distribution of the observed $\mathbf{Y}$ given $\mathbf{y}$ and a set of parameters Ω is

$$\begin{aligned}\mathrm{p}(\mathbf{Y}|\mathbf{y},\Omega) &= \prod_{b=1}^{B}\mathrm{p}(\mathbf{Y}_b|\mathbf{y}_b,\beta_b)\\ &\propto \prod_{b=1}^{B}{\beta_b}^{P/2}\exp\left\{-\frac{1}{2}\beta_b \parallel \mathbf{Y}_b-\mathbf{H}\mathbf{y}_b \parallel^2\right\}.\end{aligned} \tag{5}$$

As already described, the panchromatic image $\mathbf{x}$ is obtained by spectral averaging the unknown high resolution images $\mathbf{y}_b$. This relation is modeled as

$$\mathbf{x} = \sum_{b=1}^{B}\lambda_b\mathbf{y}_b + \mathbf{v}, \tag{6}$$

where $\lambda_b \geq 0$, $b = 1,2,\cdots,B$, are known quantities that can be obtained, as we will see later, from the sensor spectral characteristics, and $\mathbf{v}$ is the capture noise that is assumed to be Gaussian with zero mean and variance γ^{-1}. Note that, usually, $\mathbf{x}$ does not depend on all the multispectral image bands but on a subset of them, i. e., some of the λ_b's are equal to zero. For example, for Landsat ETM+ images, the panchromatic image only covers the region from the end of band 1 to the end of band 4 and the rest of the bands have no influence on $\mathbf{x}$.

Using the degradation model in Eq. (6), the distribution of the panchromatic image $\mathbf{x}$ given $\mathbf{y}$, and a set of parameters Ω is given by

$$\mathrm{p}(\mathbf{x}|\mathbf{y},\gamma) \propto \gamma^{p/2}\exp\left\{-\frac{1}{2}\gamma \parallel \mathbf{x}-\sum_{b=1}^{B}\lambda_b\mathbf{y}_b \parallel^2\right\}. \tag{7}$$

Although the estimation of the parameter vector $(\gamma,\beta_1,\ldots,\beta_B)$ can be easily incorporated in the estimation process to be described next, we will assume here that these parameters have been estimated in advance and concentrate on gaining insight into the distribution of the prior parameters. The set of hyperparameters then becomes

$$\Omega = (\alpha_1,\ldots,\alpha_B)\,. \tag{8}$$

A large part of the Bayesian literature is devoted to finding hyperprior distributions $\mathrm{p}(\Omega)$ for which $\mathrm{p}(\Omega,\mathbf{y}|\mathbf{x},\mathbf{Y})$ can be calculated in a straightforward way or can be approximated. These are the so called conjugate priors [18]. Conjugate priors have, as we will see later, the intuitive feature of allowing one to begin with a certain functional form for the prior and end up with a posterior of the same functional form, but with the parameters updated by the sample information.

Taking the above considerations about conjugate priors into account, we will assume that each of the hyperparameters in Ω has as hyperprior the gamma distribution, that is,

$$\mathrm{p}(\alpha_b(i,il) \mid a_b^o, c_b^o) \propto [\alpha_b(i,il)]^{a_b^o-1}\exp[-c_b^o\alpha_b(i,il)], \tag{9}$$

where $c_b^o > 0$ and $a_b^o > 0$ (note that the same hyperprior is assumed for all the α's in the same band). This gamma distribution has the following mean and variance

$$\mathbf{E}[\alpha_b(i,il)] = \frac{a_b^o}{c_b^o}, \quad \mathbf{var}[\alpha_b(i,il)] = \frac{a_b^o}{(c_b^o)^2}. \tag{10}$$

We will then use the following distribution on the hyperparameters

$$\mathrm{p}(\Omega) = \prod_{b=1}^{B}\prod_{i=1}^{p}\prod_{l=1}^{4}\mathrm{p}(\alpha_b(i,il) \mid a_b^o, c_b^o), \tag{11}$$

Finally, combining the first and second stage of the problem modeling we have the global distribution

$$\mathrm{p}(\Omega,\mathbf{y},\mathbf{Y},\mathbf{x}) = \mathrm{p}(\Omega)\mathrm{p}(\mathbf{y}|\Omega)\mathrm{p}(\mathbf{Y}|\mathbf{y},)\mathrm{p}(\mathbf{x}|\mathbf{y}), \tag{12}$$

where $\mathrm{p}(\Omega)$, $\mathrm{p}(\mathbf{y}|\Omega)$, $\mathrm{p}(\mathbf{Y}|\mathbf{y})$ and $\mathrm{p}(\mathbf{x}|\mathbf{y})$ have been defined in Eqs. (11), (2), (5), and (7), respectively.

Note that we have removed the dependency of $\mathrm{p}(\mathbf{Y}|\mathbf{y})$ and $\mathrm{p}(\mathbf{x}|\mathbf{y})$ on Ω because, as we have already explained, we assume that the variance of the different observation noises have been previously estimated.

4. BAYESIAN INFERENCE AND VARIATIONAL APPROXIMATION OF THE POSTERIOR DISTRIBUTION FOR SUPER RESOLUTION RECONSTRUCTION OF MULTISPECTRAL IMAGES

For our selection of hyperparameters in the previous section, the set of all unknowns is given by

$$(\Omega,\mathbf{y}) = (\alpha_1,\ldots,\alpha_B,\mathbf{y}). \tag{13}$$

As already known, the Bayesian paradigm dictates that inference on $(\Omega,\mathbf{y})$ should be based on

$$\mathrm{p}(\Omega,\mathbf{y}|\mathbf{Y},\mathbf{x}) = \frac{\mathrm{p}(\Omega,\mathbf{y},\mathbf{Y},\mathbf{x})}{\mathrm{p}(\mathbf{Y},\mathbf{x})}, \tag{14}$$

where $\mathrm{p}(\Omega,\mathbf{y},\mathbf{Y},\mathbf{x})$ is given by Eq. (12).

Since $\mathrm{p}(\Omega,\mathbf{y}|\mathbf{Y},\mathbf{x})$ can not be found in closed form, we will apply variational methods to approximate this distribution by the distribution $\mathrm{q}(\Omega,\mathbf{y})$.

The variational criterion used to find $\mathrm{q}(\Omega,\mathbf{y})$ is the minimization of the Kullback-Leibler divergence, given by [19, 13]

$$\begin{aligned} & C_{KL}(\mathrm{q}(\Omega,\mathbf{y}) \parallel \mathrm{p}(\Omega,\mathbf{y}|\mathbf{Y},\mathbf{x})) \\ &= \int_{\Omega,\mathbf{y}} \mathrm{q}(\Omega,\mathbf{y}) \log\left(\frac{\mathrm{q}(\Omega,\mathbf{y})}{\mathrm{p}(\Omega,\mathbf{y}|\mathbf{Y},\mathbf{x})}\right) d\Omega d\mathbf{y} \\ &= \int_{\Omega,\mathbf{y}} \mathrm{q}(\Omega,\mathbf{y}) \log\left(\frac{\mathrm{q}(\Omega,\mathbf{y})}{\mathrm{p}(\Omega,\mathbf{y},\mathbf{Y},\mathbf{x})}\right) d\Omega d\mathbf{y} + \text{const}, \end{aligned} \tag{15}$$

which is always non negative and equal to zero only when $\mathrm{q}(\Omega,\mathbf{y}) = \mathrm{p}(\Omega,\mathbf{y}|\mathbf{Y},\mathbf{x})$.

We choose to approximate the posterior distribution $\mathrm{p}(\Omega,\mathbf{y}|\mathbf{Y},\mathbf{x})$ by the distribution

$$\mathrm{q}(\Omega,\mathbf{y}) = \mathrm{q}(\Omega)\mathrm{q}_D(\mathbf{y}), \tag{16}$$

where $\mathrm{q}(\Omega)$ denotes distribution Ω and $\mathrm{q}_D(\mathbf{y})$ denotes a degenerate distribution on $\mathbf{y}$, that is,

$$\mathrm{q}_D(\mathbf{y}) = \begin{cases} 1 & \text{if } \mathbf{y} = \underline{\mathbf{y}} \\ 0 & \text{otherwise} \end{cases}, \tag{17}$$

where $\underline{\mathbf{y}}$ represents a known image.

Note that other distribution approximations are also possible. However, as we will see later the one used here alleviates the problem of having to estimate an enormous amount of hyperparameters.

We now proceed to find the best of these distributions in the divergence sense.

Let us assume that $\mathbf{y}^k$ is the current estimate of the multispectral image where $\mathrm{q}_D(\mathbf{y})$ is degenerate. That is, the current estimation of $\mathrm{q}_D(\mathbf{y})$ is given by

$$\mathrm{q}_D^k(\mathbf{y}) = \begin{cases} 1 & \text{if } \mathbf{y} = \mathbf{y}^k \\ 0 & \text{otherwise} \end{cases}. \tag{18}$$

Given $\mathrm{q}_D^k(\mathbf{y})$, we can obtain an estimate of $\mathrm{q}(\Omega)$ which reduces the KL-divergence by solving

$$\mathrm{q}^{k+1}(\Omega) = \arg\min_{\mathrm{q}(\Omega)} C_{KL}(\mathrm{q}(\Omega),\mathrm{q}_D^k(\mathbf{y}) \parallel \mathrm{p}(\Omega,\mathbf{y}|\mathbf{Y},\mathbf{x})). \tag{19}$$

Differentiating the integral in the right hand side of Eq. (19) with respect to $\mathrm{q}(\Omega)$ and setting it to zero we have that $\mathrm{q}^{k+1}(\Omega)$ satisfies

$$\mathrm{q}^{k+1}(\Omega) \propto \mathrm{p}(\Omega,\mathbf{y}^k,\mathbf{Y},\mathbf{x}), \tag{20}$$

which produces

$$\begin{aligned} \mathrm{q}^{k+1}(\Omega) \propto & \prod_{b=1}^{B}\prod_{i=1}^{p}\prod_{l=1}^{4} \\ & \alpha_b(i,il)^{a_b^o-1}\mathbf{e}^{-c_{\alpha_b}^o\alpha_b(i,il)}\alpha_b(i,il)^{\frac{1}{8}}\mathbf{e}^{[-\frac{1}{2}\alpha_b(i,il)[y_b(i)-y_b(il)]^2]} \end{aligned} \tag{21}$$

From Eq. (21) we have that

$$\mathrm{q}^{k+1}(\Omega) = \prod_{b=1}^{B}\prod_{i=1}^{p}\prod_{l=1}^{4}\mathrm{q}^{k+1}(\alpha_b(i,il)),$$

where

$$\mathrm{q}^{k+1}(\alpha_b(i,il)) = \mathrm{p}\left(\alpha_b(i,il) \mid a_b^o + \frac{1}{8}, \frac{1}{2}[y_b(i)-y_b(il)]^2 + c_b^o\right)$$

where the definition of the gamma distribution has been provided in Eq. (9). These distributions have the following means

$$\mathbf{E}[\alpha_b(i,il)]_{q^{k+1}(\Omega)} = \frac{a_b^o + \frac{1}{8}}{c_b^o + \frac{1}{2}[y_b^k(i)-y_b^k(il)]^2} = \alpha_b^{k+1}(i,il) \tag{22}$$

Given now $\mathrm{q}^{k+1}(\Omega)$ we can obtain an estimate of $\mathbf{y}^{k+1}$ (the value where $\mathrm{q}_D^{k+1}(\mathbf{y})$ is degenerate) which reduces the KL-divergence by solving

$$\begin{aligned} \mathbf{y}^{k+1} &= \arg\min_{\mathbf{y}}\left\{-\mathbf{E}[\log \mathrm{p}(\Omega,\mathbf{y},\mathbf{Y},\mathbf{x})]_{\mathrm{q}^{k+1}(\Omega)}\right\} \\ &= \arg\min_{\mathbf{y}}\left(\sum_{b=1}^{B}\beta_b \parallel \mathbf{Y}_b - \mathbf{H}\mathbf{y}_b \parallel^2\right. \\ &+ \sum_{b=1}^{B}\sum_{i=1}^{p}\sum_{l=1}^{4}\alpha_b^{k+1}(i,il)\,[y_b(i)-y_b(il)]^2 \\ &+ \left.\gamma \parallel \mathbf{x} - \sum_{b=1}^{B}\lambda_b\mathbf{y}_b \parallel^2\right). \end{aligned}$$

The convergence of the parameters defining the distributions $\mathrm{q}^{k+1}(\Omega)$ and $\mathrm{q}_D^{k+1}(\mathbf{y})$ can be used as stopping criterion for the iterative procedure that alternates between the estimation of both distributions.

Finally we note that Eq. (22) can be rewritten as

$$\frac{1}{\mathbf{E}[\alpha_b(i,il)]_{q^{k+1}(\Omega)}} = \mu_b\frac{c_b^o}{a_b^o} + (1-\mu_b)4[y_b^k(i)-y_b^k(il)]^2, \tag{23}$$

where

$$\mu_b = \frac{a_b^o}{a_b^o + \frac{1}{8}}. \tag{24}$$

The above equations indicate that μ_b can be understood as a normalized confidence parameter taking values in the interval $[0,1)$. That is, when it is zero no confidence is placed on the given hyperparameters, while when it is asymptotically equal to one it fully enforces the prior knowledge of the mean (no estimation of the hyperparameters is performed).

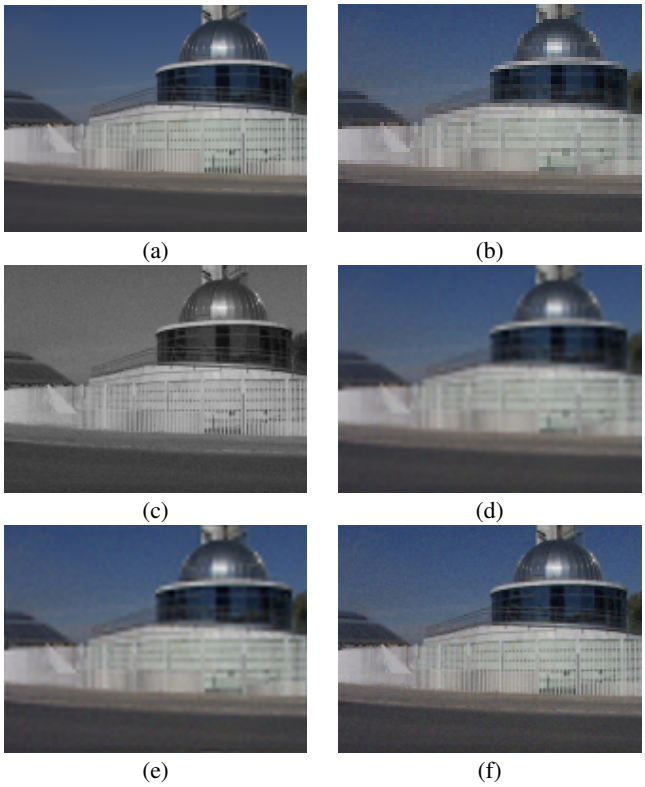

Figure 2: (a) Original HR color image; (b) Observed LR multispectral image; (c) Panchromatic image. (d) Bicubic interpolation of (b); (e) Reconstruction by the method in [20]; (f) Best reconstruction by the proposed method.

5. EXPERIMENTAL RESULTS

The proposed super resolution reconstruction algorithm has been tested on a synthetic color image and a set of Landsat ETM+ images.

In the first experiment, the color image in Fig. 2(a) was degraded using the model in Eq. (4) considering that each pixel (i,j) of the low resolution image is obtained according to (for $m = 2M$ and $n = 2N$)

$$Y_b(i,j) = \frac{1}{4} \sum_{(u,v)\in E_{i,j}} y_b(u,v) + n_b(i,j), \qquad (25)$$

where $E_{i,j}$ consists of the indices of the four high resolution pixels $E_{i,j} = \{(2i,2j),(2i+1,2j),(2i,2j+1),(2i+1,2j+1)\}$. and $n_b(i,j)$ follows a Gaussian distribution with zero mean and variance equal to four, thus obtaining the observed multispectral low resolution image depicted in Fig. 2(b). Note that the low resolution image has been resized by zero-order hold to the size of the high resolution image for displaying purposes. The panchromatic image, depicted in Fig. 2(c) was obtained from the original HR color image using the model in Eq. (6) with $\lambda_b = 1/3$, for $b = 1,2,3$, and Gaussian noise with variance 6.25.

In order to evaluate the quality of the reconstructions we used two different measures: the peak signal-to-noise ratio (PSNR) which measures the similarity between the reconstructed and original multispectral image bands, and the coefficient of correlation of the high frequency components (COR) which measures the similarity between each reconstructed multispectral image band and the panchromatic image. The COR index takes values between 0 and 1, the higher the value the better. Bicubic interpolation of each low resolution multispectral image band, the method presented in [20] and the proposed method were compared using these two objective measures and visual inspection of the resulting images.

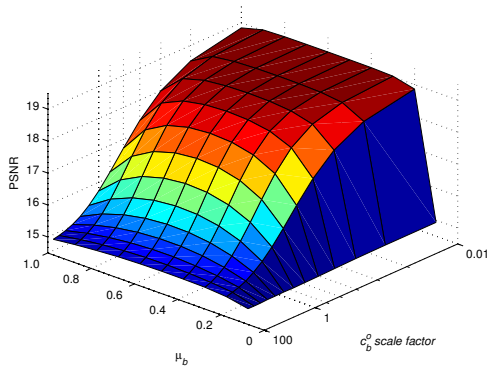

Figure 3: PSNR evolution as a function of c_b^o and μ_b.

	PSNR			COR		
band	1	2	3	1	2	3
Bicubic int.	14.7	14.7	14.7	0.55	0.56	0.56
method in [20]	15.0	15.0	15.0	0.61	0.62	0.62
proposed	18.9	19.2	19.1	0.98	0.99	0.99

Table 1: PSNR and COR values for the color image reconstructions.

The bicubic interpolation of the multispectral low resolution image (depicted in Fig. 2(d)) was used as initial reconstruction for the method in [20]. The method in [20] provided us with the reconstruction in Fig. 2(e) and with an estimate of the model parameters. In order to run the proposed method we used the estimates of β_b, $b = 1,2,3$, and γ obtained by the method in [20], and to estimate the set of parameters $\alpha_b(i,il)$ in Eq. (23) we used different values for c_b^o ranging from 10^{-2} to 10^2 times the estimate of α_b obtained by the method in [20]. We also used different values for μ_b in Eq.(24) ranging from 0 to 1. Figure 3 plots the obtained PSNR values for the different combinations of c_b^o and μ_b. The best reconstruction in terms of PSNR is depicted in Fig. 2(f). Table 1 shows the PSNR and COR values for bicubic interpolation, the method in [20], and the best reconstruction obtained by the proposed method. From this table it is clear that the proposed method outperforms all previous methods both in terms of both the PSNR and correlation of the high frequency components metrics. A visual inspection of the reconstructions makes clear that the proposed method provides much higher resolution increase than bicubic interpolation and the method in [20].

We also tested the method in real Landsat ETM+ images. Figure 4(a) depicts an 128×128 pixels false RGB color region of interest composed of bands 4, 3, and 2 of the Landsat ETM+ multispectral image and, Fig. 4(b), its corresponding 256×256 panchromatic image. As before, the multispectral image has been resized by zero-order hold to the size of the panchromatic image for displaying purposes.

The contribution of each band to the panchromatic image, that is, the values of λ_b, $b = 1,2,\ldots,4$, was obtained from the spectral response of the ETM+ sensor producing the values displayed on Table 2 (see [20] for details). Reconstructions using the method in [20] and the proposed method are shown in Fig. 4(c) and 4(d), respectively. The parameters for the proposed method were chosen as described previously for the color image. We are assuming, for this experiment, that the multispectral and panchromatic images has been already registrated. Note, however, that if this were not the case, the registation parameters could be easily included into the definition of $\mathbf{H}$ in Eq. (5). From these results it is clear that the proposed method successfully incorporates the high frequencies from

λ_1	λ_2	λ_3	λ_4
0.0078	0.2420	0.2239	0.5263

Table 2: Values for λ_b, $b = 1, \ldots, 4$.

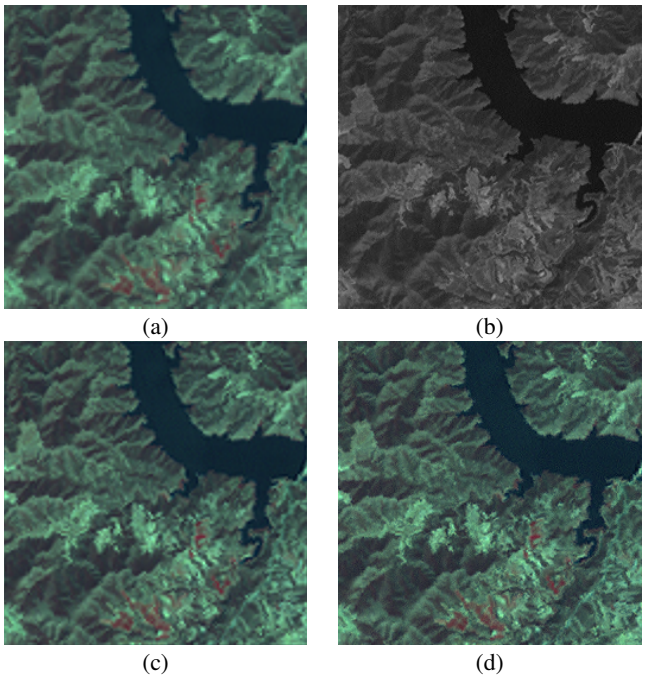

Figure 4: (a) Observed low resolution multispectral image; (b) Panchromatic image; (c) Reconstruction by the method in [20]; (d) Reconstruction by the proposed method.

the panchromatic image while preserving the spectral properties of the multispectral image.

6. CONCLUSIONS

In this paper the reconstruction of multispectral images has been formulated from a superresolution point of view. A hierarchical Bayesian framework has been presented to incorporate local prior knowledge on the expected characteristics of the multispectral images, model the observation process of both panchromatic and low resolution multispectral images, and also include information on the unknown parameters in the model in the form of hyperprior distributions has been presented. The method has been tested experimentally and it was shown to greatly outperform other methods both objectively and subjectively.

ACKNOWLEDGMENTS

This work has been partially supported by project PI040857 "Reconstrucción tridimensional de alta resolución en cámaras PET para animales pequeños", Instituto de Salud Carlos III and the Greece-Spain Integrated Action HG2004-0014.

REFERENCES

[1] W. J. Carper, T. M. Lillesand, and R. W. Kiefer, "The use of intensity-hue-saturation transformations for merging SPOT panchromatic and multispectral image data," *Phot. Eng. & Rem. Sens.*, vol. 56, no. 4, pp. 459–467, 1990.

[2] P. S. Chavez, S. Sides, and J. Anderson, "Comparison of three different methods to merge multiresolution and multispectral data: Landsat TM and SPOT panchromatic," *Phot. Eng. & Rem. Sens.*, vol. 57, no. 3, pp. 295–303, 1991.

[3] J. Nuñez, X. Otazu, O. Fors, A. Prades, V. Pala, and R. Arbiol, "Multiresolution-based image fusion with additive wavelet decomposition," *IEEE Trans on Geosc. & Rem. Sens.*, vol. 37, no. 3, pp. 1204–1211, 1999.

[4] V. Vijayaraj, "A quantitative analysis of pansharpened images," Master's thesis, Mississippi St. Univ., 2004.

[5] J. Price, "Combining multispectral data of different spatial resolution," *IEEE Trans. on Geosc. & Rem. Sens.*, vol. 37, no. 3, pp. 1199–1203, 1999.

[6] J. Park and M. Kang, "Spatially adaptive multi-resolution multispectral image fusion," *Int. Jour. of Rem. Sens.*, vol. 25, no. 23, pp. 5491–5508, 2004.

[7] M. Eismann and R. Hardie, "Hyperspectral resolution enhancement using high-resolution multispectral imaginary with arbitray response functions," *IEEE Trans. on Geosc. & Rem. Sens.*, vol. 43, no. 3, pp. 455–465, 2005.

[8] T. Akgun, Y. Altunbasak, and R. Mersereau, "Super-resolution reconstruction of hyperspectral images," *IEEE Trans. on Img. Proc.*, vol. 14, no. 11, pp. 1860–1875, 2005.

[9] R. Molina, A. K. Katsaggelos, and J. Mateos, "Bayesian and regularization methods for hyperparameter estimation in image restoration," *IEEE Trans. on Img. Proc.*, vol. 8, no. 2, pp. 231–246, 1999.

[10] M. Beal, "Variational algorithms for approximate Bayesian inference," Ph.D. dissertation, The Gatsby Computational Neuroscience Unit, University College London, 2003.

[11] M. I. Jordan, Z. Ghahramani, T. S. Jaakola, and L. K. Saul, "An introduction to variational methods for graphical models," in *Learning in Graphical Models*. MIT Press, 1998, pp. 105–162.

[12] J. Miskin, "Ensemble learning for independent component analysis," Ph.D. dissertation, Astrophysics Group, University of Cambridge, 2000.

[13] S. Kullback, *Information Theory and Statistics*. New York, Dover Publications, 1959.

[14] A. C. Likas and N. P. Galatsanos, "A variational approach for Bayesian blind image deconvolution," *IEEE Trans. on Sig. Proc.*, vol. 52, no. 8, pp. 2222–2233, 2004.

[15] R. Molina, J. Mateos, and A. Katsaggelos, "Blind deconvolution using a variational approach to parameter, image, and blur estimation," *IEEE Trans. on Img Proc.*, vol. 15, no. 12, pp. 3715–3727, 2006.

[16] J. Chandas, N. P. Galatsanos, and A. Likas, "Bayesian restoration using a new hierarchical directional continuous edge image prior," *IEEE Trans. on Image Processing*, vol. 15, pp. 2987–2997, 2006.

[17] B. D. Ripley, *Spatial Statistics*. Wiley, 1981, pp. 88 – 90.

[18] J. O. Berger, *Statistical Decision Theory and Bayesian Analysis*. New York, Springer Verlag, 1985, ch. 3 and 4.

[19] S. Kullback and R. A. Leibler, "On information and sufficiency," *Annals of Math. Stat.*, vol. 22, pp. 79–86, 1951.

[20] R. Molina, M. Vega, J. Mateos, and A. Katsaggelos, "Parameter estimation in Bayesian reconstruction of multispectral images using super resolution techniques," in *2006 International Conference on Image Processing (ICIP 2006)*, 2006, pp. 1749–1752.